European Journal of Medicinal Chemistry 76 (2014) 482–493

Contents lists available at ScienceDirect

European Journal of Medicinal Chemistry

journal homepage: http://www.elsevier.com/locate/ejmech

Original article

Celecoxib analogs bearing benzofuran moiety as cyclooxygenase-2 inhibitors: Design, synthesis and evaluation as potential anti-inflammatory agents

Ghaneya Sayed Hassan [a], Sahar Mahmoud Abou-Seri [a,*], Gehan Kamel [b], Mamdouh Moawad Ali [c]

[a] Department of Pharmaceutical Chemistry, Faculty of Pharmacy, Cairo University, Kasr El-Aini Street, Cairo 11562, Egypt
[b] Pharmacology Department, Faculty of Veterinary, Cairo University, Egypt
[c] Biochemistry Department, Division of Genetic Engineering and Biotechnology, National Research Centre, Cairo, Egypt

ARTICLE INFO

Article history:
Received 20 November 2013
Received in revised form
11 February 2014
Accepted 13 February 2014
Available online 14 February 2014

Keywords:
Celecoxib analogs
Benzofuran
Pyrazole
Anti-inflammatory agents
COX-1/COX-2 inhibitory activity

ABSTRACT

Novel series of celecoxib analogs endowed with benzofuran moiety **3a–e** and **9a–d** were synthesized and evaluated for COX-1/COX-2 inhibitory activity in vitro. The most potent and selective COX-2 inhibitors – compounds **3c**, **3d**, **3e**, **9c** and **9d** – were assessed for their anti-inflammatory activity and ulcerogenic liability in vivo. The 3-(pyridin-3-yl)pyrazole derivatives **3c** and **3e** exhibited the highest anti-inflammatory activity, that is equipotent to celecoxib. Furthermore, the tested compounds proved to have better gastric safety profile compared to celecoxib. In particular, compound **3e** demonstrated about 40% reduction in ulcerogenic potential relative to the reference drug. Finally, molecular docking simulation of the new compounds in COX-2 active site and drug likeness studies showed good agreement with the obtained pharmaco-biological results.

1. Introduction

Nonsteroidal anti-inflammatory drugs (NSAIDs) are widely used to alleviate inflammation and pains associated with many pathological conditions and are often the initial therapy for common inflammation. NSAIDs inhibit the biosynthesis of prostaglandins (PGs). In general, biosynthesis involves the conversion of arachidonic acid to prostaglandin H2 (PGH2), a reaction catalyzed by the sequential action of cyclooxygenases (COXs) [1]. Currently, it is well established that there are at least two distinct COX isoforms [1–3]. The constitutively expressed COX-1 isoform is produced in most tissues and appears to be important for the maintenance of physiological functions such as synthesis of cytoprotective PGs in the gastrointestinal tract, normal renal function, vascular homeostasis and the biosynthesis of pro-aggregatory TXA2 in blood platelets [4–7]. However, it is now believed that COX-1 is involved in a variety of pathologies that comprise many health problems as neuroinflammation, tumorgenesis, endothelial dysfunction and atherosclerosis [8]. Furthermore, platelet COX-1 is the target for novel antithrombotic agents, which affect platelet aggregation through suppression of COX-1 dependant platelet-derived TXA2 [9].

Another isoform, COX-2 is rapidly induced in inflammatory cells in response to mitogenic and proinflammatory stimuli. COX-2 makes a significant contribution to the production of inflammatory PGs, and the inhibition of COX-2 attenuates the expression of inflammatory mediators such as TNF-α, iNOS and IL-1β [10,11] and reduces the activation of transcriptional factor NF-κB which plays a crucial role in inflammation [12].

Traditional nonselective NSAIDs inhibit both COX enzymes and hence down regulate PGs formation in almost all cells and tissues. This broad inhibitory profile accounts for their anti-inflammatory activity as well as their pronounced side effects [4–7]. It was proposed that a selective inhibitor of COX-2 would be an attractive approach for the treatment of inflammatory conditions, without concomitant gastric and renal toxicity. Hence, a number of selective COX-2 inhibitors such as celecoxib, rofecoxib and valdecoxib (coxibs) have been developed and were approved for clinical use by virtue of their fewer gastrointestinal side effects compared to traditional NSAIDs. However, the long-term use of both traditional NSAIDs and coxibs has been reported to cause significant

* Corresponding author.
E-mail address: saharshaarawy_69@yahoo.com (S.M. Abou-Seri).

http://dx.doi.org/10.1016/j.ejmech.2014.02.033
0223-5234/

cardiovascular side effects [13–15]. Celecoxib has advantages in this respect; because it is not associated with an increased incidence of cardiovascular events compared with placebo and with nonselective NSAIDs [16]. There are, however, some characteristics of celecoxib that could be improved. For example, celecoxib is not effective in all patients and has some gastrointestinal side effects [17,18]. Therefore, development of new effective celecoxib analogs with improved gastrointestinal safety profile is still a necessity. Celecoxib belongs to the 1,5-diaryl pyrazole class of COX-2 inhibitors (Fig. 1). Extensive SAR studies of such class of compounds indicated that the phenyl sulfonamide moiety of the inhibitors was a major determinant for COX-2 selectivity and in vivo efficacy [19–21]. Keeping the phenyl sulfonamide moiety, two series of new celecoxib analogs were designed in which the central pyrazole ring was substituted with functionalized benzofuran moiety either at 5-position **3a**–**e** or 3-position **9a**–**d** (Fig. 1). This bulky bicyclic ring system could maximize interaction with hydrophobic residues within COX-2 active site and enhance COX-2 selectivity, as the new molecules will be too large to fit into the smaller COX-1 active site [22]. Moreover, preliminary molecular docking studies showed that the methoxy and hydroxyl substituents on benzofuran were capable of being engaged in H-bonding with essential amino acids in COX-2 active site and increased the binding affinities of the target molecules (Fig. 1). In addition, benzofuran derivatives were reported to possess anti-inflammatory activity [23–25] and exhibited promising gastro-protective effect [26–28]. Hence, the incorporation of benzofuran moiety in the designed compounds may yield new effective anti-inflammatory agents with higher safety profile compared to celecoxib.

Herein, we report the synthesis of celecoxib analogs endowed with benzofuran moiety as selective COX-2 inhibitors. The synthesized compounds were evaluated for their in vitro COX-1/COX-2 inhibitory properties as well as their in vivo anti-inflammatory activity and ulcerogenic liability. Furthermore, docking simulation and drug likeness studies were applied to identify the structural features required for COX-2 inhibitory properties of the new derivatives and to rationalize the obtained pharmaco-biological results.

2. Results and discussion

2.1. Chemistry

2.1.1. Synthesis of 4-[3-substituted-5-(6-hydroxy-4-methoxybenzofuran-5-yl)-1H-pyrazol-1-yl)]benzene sulfonamide derivatives *3a*–*c* and their 5-(6-hydroxy-4,7-dimethoxybenzofuran-5-yl) analogs *3d,e* (Scheme 1)

The 1,3-diketones **2a**–**e** were synthesized through Claisen condensation of 1-(6-hydroxy-4-methoxybenzofuran-5-yl)ethanone **1a**, or its 7-methoxy analog **1b** with ethyl acetate, ethyl trifluoroacetate or ethyl nicotinate in presence of sodium metal by applying two methods A and B. In method A, the acetophenones **1a**, **b** were refluxed with excess ethyl ester for 2 h, while in method B

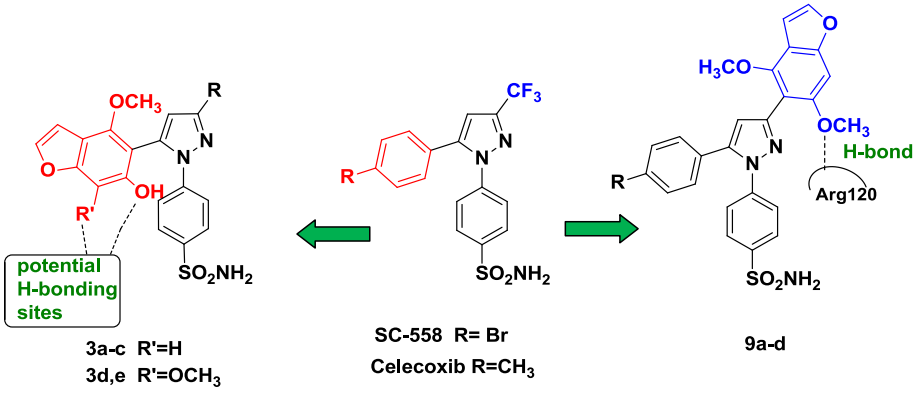

Fig. 1. Representative examples of selective COX-2 inhibitors and the designed pyrazoles **3a**–**e** and **9a**–**d**.

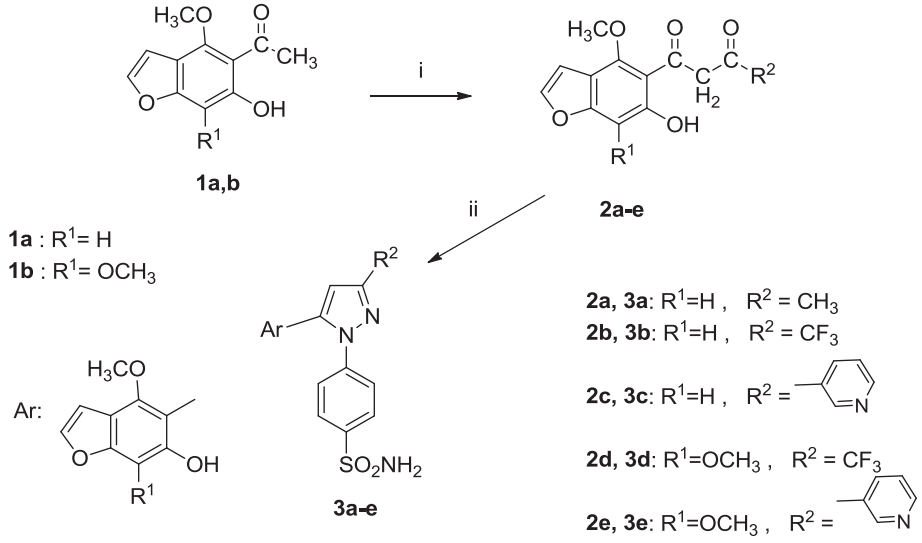

Scheme 1. Reagents and reaction conditions: i) $RCOOC_2H_5$, Na metal powder, reflux 2 h ii) $H_2NHNC_6H_4SO_2NH_2$.HCl, 6 N HCl, ethanol, reflux 8 h.

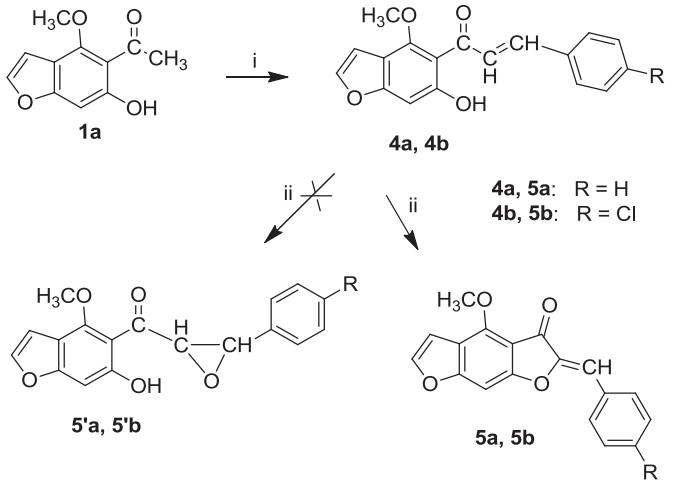

Scheme 2. : Reagents and reaction conditions: i) Ar–CHO, 30% NaOH, ethanol, 48 h ii) 30% H_2O_2, 4 N NaOH, methanol/acetone, 24 h.

equimolecular amounts of the reactants were heated in ethanol for 10 h. It is worthy note that higher yield and more pure compounds were obtained in method B. Cyclocondensation of *p*-sulfamoylphenyl hydrazine hydrochloride with 1,3-diketones **2a**–**e** in presence of hydrochloric acid and refluxing ethanol afforded the corresponding 1,5-diarylpyrazole derivatives **3a**–**e**. This reaction is regioselective and the 1,5-diarylpyrazoles could be generated almost exclusively by carrying out the condensation in acidic medium [21].

2.1.2. Synthesis of 4-[5-Aryl-3-(4,6-dimethoxybenzofuran-5-yl)-1H-pyrazol-1-yl]benzene sulfonamide derivatives **9a**–**d** (Schemes 2 and 3)

The synthetic pathway of such group of compounds should proceed through the α,β-epoxy ketone intermediates, initially obtained by oxidation of the respective chalcones **4a**,**b** as illustrated in Scheme 2, this method was utilized when little regiochemical bias was expected with 3-aryl substituent [21]. Since, it was reported [29] that 2-hydroxyphenyl chalcones underwent oxidative cyclization to aurones (2-benzylidene-1-benzofuran-3-one derivatives), accordingly, the oxidation of **4a**,**b** with hydrogen peroxide in alkaline medium into the corresponding 2-benzylidene furano[3,2-f]benzofuran-3(2*H*)-one **5a**, **b** instead of the α,β-epoxy ketones was expected (Scheme 2). Subsequently, the 1,3,5-triaryl pyrazoles **9a**–**d** were synthesized using the dimethoxy chalcone derivatives **7a**–**d** as outlined in Scheme 3. Methylation of **1a** with methyl iodide in the presence of potassium carbonate in dry acetone gave 1-(4,6-dimethoxybenzofuran-5-yl)ethanone **6**. The chalcones **7a**–**d** were prepared by conventional Claisen–Schmidt condensation reaction of **6** with different aldehydes in the presence of 30% sodium hydroxide in ethanol. Treatment of α,β-unsaturated ketones **7a**–**d** with 30% hydrogen peroxide under basic conditions yielded the α,β-epoxy ketone intermediates **8a**–**d** via Weitz–Scheffer oxidation reaction [30,31]. Finally, reacting **8a**–**d** with *p*-sulfamoylphenylhydrazine hydrochloride in boiling ethanol acidified with acetic acid, led to the formation of 4-[5-aryl-3-(4,6-dimethoxybenzofuran-5-yl)-1*H*-pyrazol-1-yl]benzenesulfonamide derivatives **9a**–**d**.

2.2. Pharmacobiological activity

2.2.1. In vitro cyclooxygenase (COX) inhibition assay

The target of the biological activity tests was to study the ability of tested compounds to inhibit ovine COX-1 and human recombinant COX-2 using an enzyme immunoassay (EIA) kit. The efficacies of tested compounds were determined as the concentration causing 50% enzyme inhibition (IC_{50}); Table 1. All the tested compounds showed no inhibition of COX-1 up to 50 μM. Meanwhile, potent COX-2 inhibitory activity was observed with compounds **3c**, **3d**, **3e**, **9c** and **9d** with IC_{50} 0.40, 0.52, 0.36, 0.46, 0.34 μM respectively. Moreover, the selectivity indices (SI values) – defined as IC_{50} (COX-1)/IC_{50} (COX-2) – were calculated and compared with that of the standard selective COX-2 inhibitor; celecoxib. In the assay system, the IC_{50} values of celecoxib on COX-1 and COX-2 were determined to be >50 and 0.28 μM, indicating that celecoxib is a

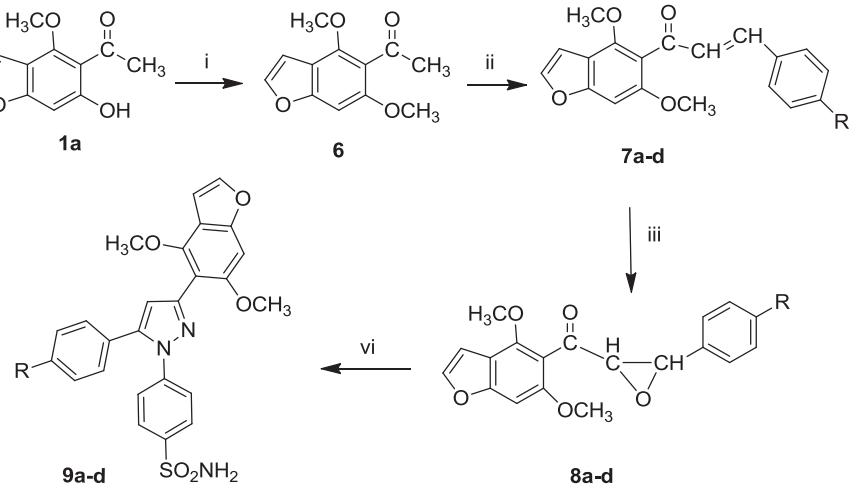

Scheme 3. Reagents and reaction conditions: i) CH_3I, anhy. K_2CO_3, dry acetone, reflux 24 h, ii) Ar–CHO, 30% NaOH, ethanol, 48 h, iii) 30% H_2O_2, 4 N NaOH, methanol/acetone, 24 h, iv) $H_2NHNC_6H_4SO_2NH_2$.HCl, ethanol, acetic acid, reflux 6 h.

Table 1
Data of the in vitro COX-1/COX-2 enzyme inhibition assay of the designed compounds.

Compound No.	IC_{50} (μM)[a]		SI[b]
	COX-1	COX-2	
3a	>50	7.50	>6.67
3b	>50	7	>7.14
3c	>50	0.40	>125
3d	>50	0.52	>96.15
3e	>50	0.36	>138.90
9a	>50	35	>1.43
9b	>50	26	>1.93
9c	>50	0.46	>108.70
9d	>50	0.34	>147.06
Celecoxib	>50	0.28	>178.57

[a] IC_{50} value is the compound concentration required to produce 50% inhibition of COX-1 or COX-2 for means of two determinations and deviation from the mean is <10% of the mean value.
[b] Selectivity index IC_{50} (COX-1)/IC_{50} (COX-2).

selective COX-2 inhibitor (SI > 178.57). The results revealed that most of the compounds showed potent inhibition against COX-2 (IC_{50}: 0.34–7.50 μM) and were inactive against COX-1 (IC_{50} > 50 μM) as listed in Table 1. Nearly, five compounds (**3c**, **3d**, **3e**, **9c** and **9d**) were found to be potent and selective similar to celecoxib against COX-2.

The structure activity data acquired showed that the pyrazole C-3 substituent was a determinant of COX-2 inhibitory potency and selectivity of the 5-(6-hydroxy-4-methoxybenzofuran-5-yl)pyrazole derivatives **3a**–**c**. The celecoxib analogue **3b** with trifluoromethyl substituent displayed moderate activity compared to the reference drug with IC_{50} = 7.0 μM. Changing the trifluoromethyl group in **3b** into methyl group in **3a** led to minor decrease in COX-2 inhibition (IC_{50} = 7.50 μM). Conversely, a remarkable improve in enzyme inhibitory activity as well as selectivity was observed upon replacement of the same group with pyridin-3-yl moiety in **3c** (IC_{50} = 0.40 μM, SI > 125.00). On the other hand, both COX-2 potency and selectivity of **3b** were found to increase also, by introducing an extra methoxy group on C-7 of the benzofuran moiety (**3d**; IC_{50} = 0.52 μM, SI > 96.15). Interestingly, applying the same structural modification to **3c** produced **3e** with minor improvement in COX-2 inhibitory effect (IC_{50} = 0.36 μM, SI > 138.90).

Considering the 5-[4-(un) substituted phenyl]-3-(4,6-dimethoxybenzofuran-5-yl)pyrazole derivatives **9a**–**d**, it seems that the *p*-substituent on the phenyl ring modulated the COX-2 inhibitory potency of these compounds. In general, molecules possessing *p*-electronegative substituent **9b**–**d** were more potent COX-2 inhibitors than the unsubstituted phenyl counterpart **9a** (CF_3 > F > Cl > H). Although, compound **9b** with *p*-chlorophenyl moiety proved to be weak and nonselective COX-2 inhibitor (IC_{50} = 26.00 μM, SI > 1.93), grafting the more electronegative fluorine atom in **9c** or trifluoromethyl group in **9d** to the phenyl ring of **9a** induced COX-2 selectivity and resulted in approximately 77 and 100 fold boost in potency, respectively (**9c**: IC_{50} = 0.34 μM, SI > 108.70; **9d**: IC_{50} = 0.34 μM, SI > 147.06). The difference in electronegativity between fluorine and carbon creates a large dipole moment in this bond. This dipole may contribute to the molecule's ability to be engaged in intermolecular interactions with COX-2 active site.

2.2.2. In vivo anti-inflammatory activity against formalin induced rat paw edema

Anti-inflammatory activity of compounds **3c**, **3d**, **3e**, **9c** and **9d**, which showed the highest inhibitory potency and selectivity for COX-2 isozyme in vitro, was evaluated by employing the standard formalin-induced foot paw edema method in rats using celecoxib as a reference drug [32]. Mean changes in paw edema thickness after 1/2, 1, 2 and 3 h from induction of inflammation and percentages of edema inhibition given by the tested compounds and celecoxib at 50 mg/kg body weight dose level are depicted in Table 2. All the tested compounds were found to possess potent anti-inflammatory activity (83.6–100% reduction in inflammation after 3 h). The 3-(pyridin-3-yl)pyrazole derivatives **3c** and **3e** showed the highest in vivo activity with edema inhibition % = 90 after 1/2 h to 100 after 3 h, that was equipotent to the reference drug celecoxib (edema inhibition % = 94 after 1/2 h to 100 after 3 h). Moreover, compounds **3d**, **9c** and the most potent COX-2 inhibitor **9d** exhibited impressive anti-inflammatory effect (edema inhibition % = 91.8, 83.61 and 91.8 after 3 h, respectively). The higher in vivo potency of pyridine containing derivatives **3c** and **3e** compared to compounds **3d**, **9c** and **9d** reflects their better pharmacokinetic properties and higher systemic bioavailability. This might be partly due to their enhanced aqueous solubility and in consequence, increased rate of dissolution as a perquisite parameter for absorption through different biological membranes.

2.2.3. Ulcerogenic liability

The ulcerogenic potential of the most potent COX-2 inhibitors **3c**, **3d**, **3e**, **9c** and **9d** (50 mg/kg) was evaluated according to Meshali's method [33] and the ulcer index was calculated according to Robert's method [34]. The ulcerogenic effect was compared to celecoxib (50 mg/kg) and the classical NSAID ibuprofen (25 mg/kg) [35].[1] From the data obtained, Table 3, it has been observed that all the synthesized pyrazoles endowed with benzofuran moiety caused less gastric ulceration effect (ulcer index of compound **3c**: 13.82 ± 0.62; **3d**: 11.56 ± 0.54; **3e**: 10.50 ± 0.63; **9c**: 11.75 ± 0.63 and **9d**: 10.50 ± 0.59) in the experimental animals, compared to that of the standards, ibuprofen (ulcer index 22.32 ± 0.86) and celecoxib (ulcer index 16.12 ± 0.86).

Therefore, the potential value of these compounds as anti-inflammatory agents is that they have highly better safety margin on gastric mucosa than ibuprofen. These promising ulcer protective properties of the designed pyrazole-benzofuran derivatives greatly supported our main objective to avoid gastric injuries caused by COX-1 inhibition. Moreover, compound **3e** with best overall profile in animal efficacy model showed about 40% reduction in ulcerogenic potential versus celecoxib. Hence, this successful result supported the aim of the present work to develop novel series of celecoxib analogs bearing benzofuran moiety as COX-2 inhibitors with diminished gastrointestinal side effects.

2.3. Molecular modeling

To further explore the mechanism of interaction of the newly synthesized compounds within COX-2 active site and to account for the obtained biological results docking analysis was carried out. Docking of the new inhibitors and the reference drug celecoxib into the crystal structure of COX-2 enzyme catalytic domain in complex with the diaryl heterocyclic inhibitor SC-558 [PDB ID code 6COX] [36] was performed using Molecular Operating Environment MOE version 2008.10 [37]. The most stable docking model was selected according to the best scored conformation predicted by the MOE scoring function, Table 4.

[1] The animal dose of the reference drugs was calculated relative to human dose using reported equivalent surface area dosage conversion factors which correlate the dosage of different species [35]. Calculations were made considering the highest adult dose of celecoxib (400 mg) and the lowest adult dose of ibuprofen (200 mg) to demonstrate the high safety margin of the new compounds.

Table 2
Anti-inflammatory activity of the tested compounds and celecoxib (50 mg/kg p.o.) against formalin-induced paw edema in rats.

Treatment	Increase in paw thickness (mm)				Edema inhibition %			
	30 min	1 h	2 h	3 h	30 min	1 h	2 h	3 h
Control	0.54 ± 0.018	0.57 ± 0.016	0.58 ± 0.019	0.61 ± 0.022	0	0	0	0
Celecoxib	0.03 ± 0.0027[a]	0	0	0	94.44	100	100	100
3c	0.05 ± 0.007[a]	0.02 ± 0.001[a]	0	0	90.14	96.19	100	100
3d	0.15 ± 0.012[a]	0.12 ± 0.008[a]	0.07 ± 0.004[a]	0.05 ± 0.003[a]	72.22	78.95	87.93	91.80
3e	0.05 ± 0.006[a]	0.02 ± 0.003[a]	0	0	90.74	96.49	100	100
9c	0.11 ± 0.018[a]	0.10 ± 0.018[a]	0.10 ± 0.019[a]	0.10 ± 0.019[a]	79.63	82.46	82.76	83.61
9d	0.18 ± 0.034[a]	0.13 ± 0.022[a]	0.03 ± 0.006[a]	0.05 ± 0.01[a]	66.67	77.19	94.83	91.80

Results are means of five experiments ± S.E.
[a] Significantly different from the control value at $p < 0.01$.

Table 3
Ulcerogenic effect of celecoxib, **3c**, **3d**, **3e**, **9c** and **9d** in rats (50 mg/kg) and ibuprofen (25 mg/kg).

Treatment	No. of animals with ulcers	% Incidence divided by 10	Average number of ulcers	Average severity (Ulcer score)	Ulcer index
Control	0/5	0	0	0	0
Celecoxib	5/5	10	5	1.12	16.12 ± 0.86
Ibuprofen	5/5	10	10	2.32	22.32 ± 0.86
3c	5/5	10	3	0.82	13.82 ± 0.62[b]
3d	4/5	8	3	0.56	11.56 ± 0.54[a,b]
3e	4/5	8	2	0.5	10.50 ± 0.63[a,b]
9c	4/5	8	3	0.75	11.75 ± 0.63[a,b]
9d	4/5	8	2	0.50	10.50 ± 0.59[a,b]

[a] Significantly different from celecoxib value at $p < 0.01$.
[b] Significantly different ibuprofen value at $p < 0.01$. Results are means of five experiments ± S.E.

Visual inspection of the protein complex reveals that COX active site has three deferential regions: the carboxylate site at entrance of COX active site which appears as a constriction composed of three hydrophilic residues Arg 120, Tyr 355 and Glu 524 arranged to form H-bond network. The entrance leads to a long hydrophobic channel that extends deep into the interior of the catalytic domain. In COX-2, this channel forks to a primary hydrophobic pocket and side pocket. The primary pocket is defined by the amino acids Tyr 385, Trp 387, Phe 518 and Ser 530. The side pocket (selectivity site) is located above Arg 120, Tyr 355, Glu 524 constriction; this pocket is bordered by Val 523 and contains the conserved residue His 90 and the nonconserved residue Arg 513 [38].

To validate the docking protocol, the co-crystallized ligand was redocked into COX-2 active site and the docking pose was compared with the initial pose using root mean square deviation (RMSD). SC-558 docked almost at the same position (RMSD = 0.218 Å) with docking score of −14.11 kcal/mol (Table 4). The bromophenyl ring is bound in the primary hydrophobic pocket. The trifluoromethyl group is bound in an adjacent pocket formed by Val 116, Val 349, Tyr 355, Leu 359 and Leu 531. The phenyl sulfonamide moiety is inserted in the side pocket where the sulfonamide group H-bonded with His 90 and Arg 513 (2.90 and 2.70 Å respectively) Fig. 2A, such interactions are almost essential for COX-2 inhibitory activity [36,38]. Also, the selectivity of SC-558 seems to result from the binding of the sulfonamide group to this pocket which is more restricted in COX-1 [38]. Similar to SC-558, celecoxib was docked into COX-2 active site revealing the same orientation and binding behavior (Fig. 2A, Table 4).

2.3.1. *Docking of 4-[3-substituted-5-(6-hydroxy-4-methoxybenzofuran-5-yl)-1H-pyrazol-1-yl)]benzene sulfonamide derivatives **3a**–**c** and their 5-(6-hydroxy-4,7-dimethoxybenzofuran-5-yl) analogs **3d**,**e***

Docking calculations showed that the new pyrazoles (**3a**–**e**) bound to COX-2 binding site with the same orientation of the co-crystalized ligand SC-558 and celecoxib. The central pyrazole is involved in arene–cation interaction with the guanidinium side chain of Arg 120. The benzofuran moeity is positioned in the primary hydrophobic pocket occupied by the bromophenyl ring of SC-558 and is stabilized by hydrophobic interaction with Leu 384, Tyr 385, Trp 387 and Phe 518 with contribution from the backbone of Leu 531. Also, the N^1-phenyl sulfonamide is oriented toward the side pocket, where one of the sulfonamide oxygen atoms is linked by H-bond to Arg 513, while the amide nitrogen is H-bonded to His 90 (Fig. 2B–D, Table 4).

Moreover, the pyridine ring of **3c** was in van der Waal contact with side chains of Val 116, Val 439, Tyr 355 and Leu 531 amino acids, while its benzofuran moiety was pushed more deep in the hydrophobic pocket compared to the same moiety in **3a** and **3b**. Thus, the difference in relative position of benzofuran enabled H-bonding between 6-hydroxy group and Val 523 (2.80 Å) (Fig. 2B). On the other hand, the docked posses of compounds **3d** and **3e** with extra methoxy group on C-7 of the benzofuran moiety (Fig. 2C and D) illustrated the potential of the 7-methoxy oxygen to be involved in two H-bonds with the side chain hydroxyl groups of Ser 530 and Try 385 amino acids. Several structural and functional evidences supported that Try 385 and Ser 530 chelation is critical for inhibition of COX-2 by the clinically used NSAIDs, diclofenac, piroxicam and nimesulide [39]. Accordingly, the lack of additional H-bond interactions with Val 523 in case of **3c** or with Ser 530 and Try 385 for the analogs **3d** and **3e** might be responsible for the reduced COX-2 inhibitory activity of **3a** and **3b**.

2.3.2. *Docking of 4-[5-aryl-3-(4,6-dimethoxybenzofuran-5-yl)-1H-pyrazol-1-yl]benzene sulfonamide derivatives **9a**–**d***

The docking models of the pyrazoles **9a**–**d** showed that the compounds are typically positioned in COX-2 active site with their substituted phenyl ring projecting up into the primary hydrophobic pocket toward Try 385 and Trp 387. Meanwhile, the N^1 phenyl sulfonamide is directed toward the side pocket with the sulfonamide functionality embedded in the selectivity site forming two H-bonding interactions with His 90 and Arg 513, Table 4. The 4,6-

Table 4
Docking score and bond interactions of **SC-558**, celecoxib and synthesized compounds with amino acids of COX-2.

Compound	Docking score (kcal/mol)	No. of H-bonds	Distance (Å)	Amino acid involved	Molecular structure
SC-558	−14.11	2	2.90	His 90	NH of SO_2NH_2
			2.70	Arg 513	O of SO_2NH_2
Celecoxib	−16.35	2	2.91	His 90	NH of SO_2NH_2
			2.64	Arg 513	O of SO_2NH_2
3a	−16.66	2	2.90	His 90	N of SO_2NH_2
			2.46	Arg 513	O of SO_2NH_2
3b	−15.23	2	2.89	His 90	N of SO_2NH_2
			2.42	Arg 513	O of SO_2NH_2
3c	−17.04	3	2.89	His 90	N of SO_2NH_2
			2.43	Arg 513	O of SO_2NH_2
			2.80	Val 523	H of 6-OH
3d	−18.19	4	2.88	His 90	N of SO_2NH_2
			2.45	Arg 513	O of SO_2NH_2
			2.47	Ser 530	O of 7-OCH_3
			2.92	Tyr 385	O of 7-OCH_3
3e	−18.51	4	2.19	His 90	N of SO_2NH_2
			2.48	Arg 513	O of SO_2NH_2
			2.50	Ser 530	O of 7-OCH_3
			2.76	Tyr 385	O of 7-OCH_3
9a	−17.84	3	2.88	His 90	NH of SO_2NH_2
			2.52	Arg 120	O of 6-OCH_3
			2.71	Arg 513	O of SO_2NH_2
9b	−17.09	3	2.99	His 90	NH of SO_2NH_2
			2.96	Arg 120	O of 6-OCH_3
			2.61	Arg 513	O of SO_2NH_2
9c	−18.82	3	2.98	His 90	NH of SO_2NH_2
			2.52	Arg 120	O of 6-OCH_3
			2.61	Arg 513	O of SO_2NH_2
9d	−20.18	3	2.96	His 90	NH of SO_2NH_2
			2.49	Arg 120	O of 6-OCH_3
			2.66	Arg 513	O of SO_2NH_2

dimethoxy benzofuran moiety at C-3 is oriented to the carboxylate site of the enzyme in correspondence with the trifluoromethyl group of SC-558. This orientation involved hydrogen bonding of the oxygen atom of the 6-methoxy group with Arg 120. Furthermore, Ile 345, Val 349 and Leu 531 were within close van der Waal contact with benzofuran moiety (Fig. 3A–B).

It was interesting to note that *the structural* analogs **9a–d** showed strikingly different levels of activity in the enzyme assay. The profound enhancement in COX-2 inhibitory effect of the fluorophenyl and trifluoromethyl phenyl derivatives **9c** and **9d** suggested that they bound to the enzyme in such away to maximize their interaction with the binding site. As seen in Table 4, these compounds had the highest binding affinities (docking score: −18.82 and −20.18 kcal/mol). This may be attributed to the highly electronegative nature of fluorine atom or trifluoromethyl group which led to a more efficient π–π stack interaction of the phenyl ring with Try 385 and Trp 387 [40,41]. Also, the difference in electronegativity between fluorine and carbon creates a large dipole moment in this bond. This dipole may contribute to the molecule's ability to be engaged in intermolecular interactions with COX-2 active site [42,43].

2.4. ADME profiling

The bioavailability of the reference drug celecoxib and the most active compounds **3c–e, 9c** and **9d** was assessed using mipc – Molinspiration Property Calculator [44]. In particular, we calculated the compliance of compounds to Lipinski's "rule of five" [45]. The rule describes molecular properties important for drug's pharmacokinetics in the human body, including their absorption, distribution, metabolism and elimination (ADME) and is used to insure that drug-like physicochemical properties are maintained during drug design. These simple rules state that oral bioavailability is likely to occur if at least three of the following rules are obeyed: molecular weight less than 500 Da; no more than five hydrogen bond donors and less than 10 hydrogen bond acceptors; and calculated octanol–water partition coefficient (c log P) not greater than 5 [45]. Also, topological polar surface area (TPSA) and the number of rotatable bonds have been found to be very good descriptors of oral bioavailability of drugs. Compounds which meet the two criteria of ten or fewer rotatable bonds and polar surface area equal to or less than 140 $Å^2$ are predicted to have good oral bioavailability [44]. The calculated parameters (Table 5) showed good bioavailability of studied compounds. Compounds **3c**, **3d** and **9c** fulfilled all rules, similar to the clinically used drug celecoxib. Meanwhile, compound **3e** had slightly large TPSA (142.72 $Å^2$) and compound **9d** was violated from the rule of five by one represented by molecular weight value. Theoretically, these compounds should present good passive oral absorption and differences in their bioactivity cannot be attributed to these properties.

Compounds **9d**, **3e**, **3c**, **9c** and **3d** which showed the highest inhibitory activity and selectivity for COX-2 enzyme in the in vitro assay (IC_{50} = 0.34, 0.36, 0.40, 0.46, 0.52 μM respectively), exhibited anti-inflammatory activity with edema inhibition % (66.67, 90.74, 90.14, 81.84 and 72.22 respectively) after 30 min. The high potency and the rapid onset of action of 3-(pyridin-3-yl)pyrazoles **3e** and **3c** might be attributed to their enhanced aqueous solubility (miLog*P*: 2.61 and 2.62, respectively). Aqueous solubility governs both the rate of dissolution of the compound and the maximum concentration reached in the gastrointestinal fluid and may be the main factor ensuring a good level of distribution of these compounds in vivo [46]. Besides, partition coefficients of compounds **3e** and **3c** were measured experimentally using reversed-phase thin layer chromatography [47]. The determined log *P* values were 2.48 and 2.21, respectively, which asserted the hydrophilic characteristics of compounds.

3. Conclusion

The present study reported the design and synthesis of novel celecoxib analogs endowed with benzofuran moiety as selective COX-2 inhibitors. The synthesized compounds were evaluated for their COX-1/COX-2 inhibitory activity in vitro. Compounds **3c**, **3d**, **3e**, **9c** and **9d** were found to be potent and selective COX-2 inhibitors (IC_{50}: 0.34–0.52 μM) and were inactive against COX-1 (IC_{50} > 50 μM). SAR was discussed in terms of the enzyme inhibitory activity and was supported by molecular docking simulations and analysis of the binding modes of the new inhibitors within COX-2 active site. The H-bonding capability seems to be the most crucial factor affecting the activity of a series 5-(6-hydroxy-4-methoxybenzofuran-5-yl)pyrazoles **3a–c** and their 5-(6-hydroxy-4,7-dimethoxybenzofuran-5-yl) analogs **3d,e**. Meanwhile, the electronic effect (electronegativity) of *p*-substituent on the phenyl ring exerted the major influence on the COX-2 inhibitory potency of 5-[4-(un) substituted phenyl]-3-(4,6-dimethoxybenzofuran-5-yl) pyrazole derivatives **9a–d**. In addition, the most potent COX-2 inhibitors **3c**, **3d**, **3e**, **9c** and **9d** were assessed for their anti-inflammatory activity and ulcerogenic liability in vivo. Interestingly, the 3-(pyridin-3-yl)pyrazole derivatives **3c** and **3e** exhibited the highest anti-inflammatory activity, that is equipotent to the reference drug celecoxib. These results suggested a contributory role of C-3 pyridin-3-yl in improving the anti-inflammatory efficiency in animal models. Moreover, the tested compounds proved to have better gastrointestinal safety profile compared to celecoxib.

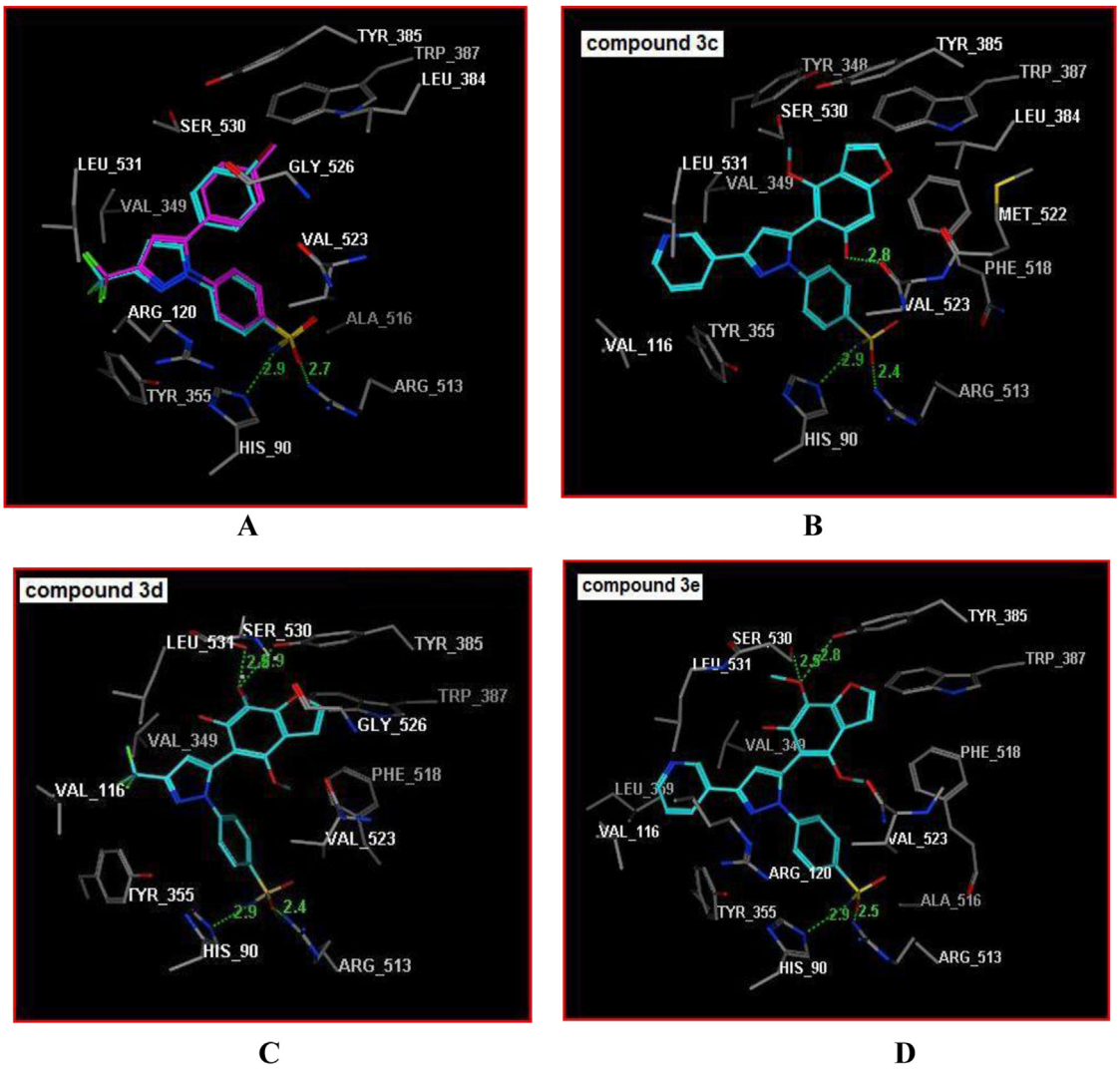

Fig. 2. (A) Superimposition of **SC-558** (blue) and celecoxib (purple) docked in the active site of COX-2 enzyme. (B–D) Docking poses of the potent 5-(6-Hydroxy-4-methoxybenzofuran-5-yl) pyrazole derivative **3c** (B) and 5-(6-Hydroxy-4,7-dimethoxybenzofuran-5-yl) pyrazole derivatives **3d** (C) and **3e** (D) within COX-2 active site. (For interpretation of the references to colour in this figure legend, the reader is referred to the web version of this article.)

In particular, compound **3e** demonstrated about 40% reduction in ulcerogenic potential relative to the reference drug, which makes it a good lead-candidate for further optimization and development of potent and safe anti-inflammatory agents.

4. Experimental

4.1. Chemistry

Melting points were determined by open capillary tube method using Gallen Kamp melting point apparatus MFB-595-010M (Gallen Kamp, London, England) and were uncorrected. Microanalysis was carried out at the regional center for microbiology and biotechnology, Al-Azhar University; Organic Microanalyses Section, Central Laboratory, National Research Center and the Micro Analytical Center, Faculty of Science, Cairo University. Infrared Spectra were recorded as potassium bromide discs on Schimadzu FT-IR 8400S spectrophotometer (Shimadzu, Kyoto, Japan) and expressed in wave number (cm^{-1}). The NMR spectra were recorded on a Varian Mercury VX-300 NMR spectrometer. ^1H spectra were run at 300 MHz and ^{13}C spectra were run at 75.46 MHz in deuterated chloroform ($CDCl_3$) or dimethyl sulphoxide (DMSO-d_6). Chemical shifts are quoted in δ as parts per million (*ppm*) downfield from tetramethylsilane (TMS) as internal standard. Mass spectra were recorded using Hewlett Packard Varian (Varian, Polo, USA) and Shimadzu Gas Chromatograph Mass spectrometer-QP 1000 EX (Shimadzu, Kyoto, Japan). TLC were carried out using Art.DC-Plastikfolien, Kieselgel 60 F254 sheets (Merck, Darmstadt, Germany), the developing solvents were $CCl_4/CH_3COOC_2H_5$ (9:1) or (4:1) and the spots were visualized at 366, 254 nm by UV Vilber Lourmat 77202 (Vilber, Marne La Vallee, France).

Compounds **1a**, **1b** [48], **2a** [49], **2c**, **2e** [50], **4a, 4b, 5a**, **6** [51] and **7a** [52] were prepared according to reported procedures.

4.1.1. General procedure for the synthesis of 4,4,4-trifluoro-1-(6-hydroxy-4-methoxybenzofuran-5-yl)butane-1,3-dione derivatives (**2b**) and 4,4,4-trifluoro-1-(6-hydroxy-4,7-dimethoxybenzofuran-5-yl)butane-1,3-dione (**2d**)

4.1.1.1. Method A. A solution of **1a** or **1b** (10 mmol) in ethyl trifluoroacetate (50 mmol, 7.10 g, 6.0 ml) was treated with (25 mmol,

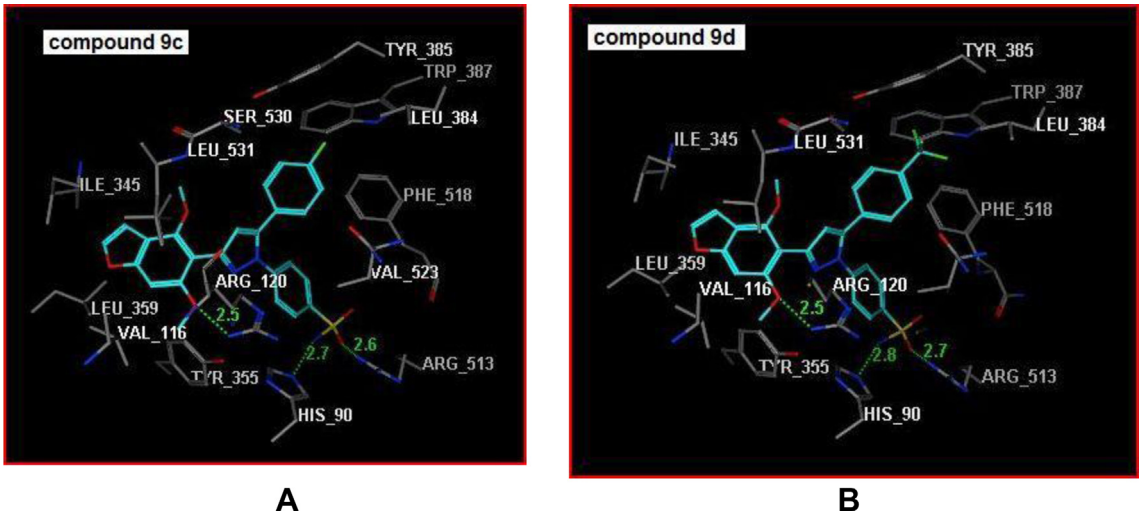

Fig. 3. Docking poses of the most potent 3-(4,6-dimethoxybenzofuran-5-yl)pyrazole derivatives **9c** (A) and **9d** (B) in the active site of COX-2 enzyme.

0.57 g) powdered sodium (prepared under toluene). After the initial reaction subsided, the mixture was refluxed for 2 h. The reaction mixture was left to stand overnight, treated with ice-water and extracted with ether. The aqueous solution, after being freed from ether by a stream of air was acidified with acetic acid and extracted with $CHCl_3$. The chloroformic extract was filtered through anhydrous Na_2SO_4 and the filtrate was evaporated under vacuum. The residue was crystallized from $CHCl_3$/ether to give **2b** and **2d**, respectively.

4.1.1.2. Method B. To a solution of sodium (30 mmol, 0.69 g) in methanol (20 ml), ethyl trifluoroacetate (20 mmol, 2.84 g, 2.4 ml) was added. After 30 min, a solution of **1a** or **1b** (20 mmol) in methanol (5 ml) was added. The resulting reaction mixture was stirred for 10 h at 80 °C then evaporated to dryness. The obtained sodium salt was dissolved in water (10 ml), acidified with acetic acid and extracted several times with ethyl acetate. The organic layer was dried over anhydrous $MgSO_4$ and evaporated under vacuum to give **2b** and **2d**, respectively.

*4.1.1.3. 4,4,4-Trifluoro-1-(6-hydroxy-4-methoxybenzofuran-5-yl) butane-1,3-dione (**2b**).* Yield 50% (method A) and 60% (method B), m.p. 180–182 °C. IR (KBr, cm^{-1}): 3128 (OH), 1701, 1662 (2 C=O). ^1H NMR ($CDCl_3$) δ *ppm*: 4.14 (s, 2H, $COCH_2CO$), 4.23 (s, 3H, OCH_3), 6.72 (s, 1H, H-7 benzofuran), 6.89 (d, 1H, H-3 benzofuran, J = 2.4 Hz), 7.49 (d, 1H, H-2 benzofuran, J = 2.4 Hz), 10.50 (s, 1H, OH, exch. D_2O). MS, *m/z*: 302 [M^+]. Anal. Calcd. for $C_{13}H_9F_3O_5$ (302.20): C, 51.67; H, 3.00. Found: C, 51.52; H, 2.72.

*4.1.1.4. 4,4,4-Trifluoro-1-(6-hydroxy-4,7-dimethoxybenzofuran-5-yl) butane-1,3-dione (**2d**).* Yield 55% (method A) and 63% (method B), m.p. 216–218 °C. IR (KBr, cm^{-1}): 3132 (OH), 1700, 1651 (2C=O). ^1H NMR ($CDCl_3$) δ *ppm*: 3.32 (s, 3H, OCH_3), 3.83 (s, 3H, OCH_3), 4.01 (s, 2H, $COCH_2CO$), 7.15 (d, 1H, H-3 benzofuran, J = 2.4 Hz), 7.86 (d, 1H, H-2 benzofuran, J = 2.4 Hz), 11.54 (s, 1H, OH, exch. D_2O). ^{13}C NMR (DMSO) δ: 33.5 (CH_2), 61.0 (OCH_3), 61.1 (OCH_3), 106.4 (C-3 and C-3a), 111.5 (C-5), 114.2 (CF_3), 128.7 (C-7), 145.2 (C-2 and C-4), 149.2 (C-7a), 150.9 (C-6), 204.2 (2C=O). MS, *m/z*: 333 [M^+ +1]. Anal. Calcd. for $C_{14}H_{11}F_3O_6$ (332.23): C, 50.61; H, 3.34. Found: C, 50.72; H, 3.14.

*4.1.2. General procedure for the synthesis of 4-[3-substituted-5-(6-hydroxy-4-methoxybenzofuran-5-yl)-1H-pyrazol-1-yl)]benzene sulfonamide derivatives (**3a**–**c**) and 4-[3-substituted-5-(6-hydroxy-4,7-dimethoxybenzofuran-5-yl)-1H-pyrazol-1-yl)]benzene sulfonamide derivatives (3**d**,**e**)*

The appropriate β-diketone derivative **2a**–**e** (10 mmol) was added to a stirred solution of *p*-sulfamoylphenylhydrazine hydrochloride (11 mmol, 2.46 g) in ethanol (40 ml) and 6 N HCl (22 mmol, 3.7 ml). The mixture was heated to reflux and stirred for 8 h. After cooling to room temperature, the reaction mixture was concentrated under vacuum. The residue was taken up with ethyl acetate and washed with water, dried over anhydrous $MgSO_4$, filtered, and evaporated under vacuum. The residue was crystallized from ethanol.

*4.1.2.1. 4-[5-(6-Hydroxy-4-methoxybenzofuran-5-yl)-3-methyl-1H-pyrazol-1-yl]benzene sulfonamide (**3a**).* Yield 55%, m.p. 112–113 °C. IR (KBr, cm^{-1}): 3329, 3248 (NH_2), 3151 (OH), 1624 (C=N), 1338, 1153 (SO_2). ^1H NMR ($CDCl_3$) δ *ppm*: 1.55 (s, 2H, NH_2, exch. D_2O), 2.72 (s, 3H, CH_3), 4.22 (s, 3H, OCH_3), 4.94 (s, 1H, H-4 pyrazole), 6.73 (s, 1H, H-7 benzofuran), 7.24 (d, 1H, H-3 benzofuran, J = 1.8 Hz), 7.48 (d, 1H, H-2 benzofuran, J = 1.8 Hz), 7.76 (d, 2H, H-2 and H-6 $ArSO_2NH_2$, J = 8.7 Hz), 8.13 (d, 2H, H-3 and H-5 $ArSO_2NH_2$, J = 8.4 Hz), 10.80 (s, 1H, OH, exch. D_2O). MS, *m/z*: 399 [M^+]. Anal. Calcd. for $C_{19}H_{17}N_3O_5S$ (399.42): C, 57.13; H, 4.29; N, 10.52; S, 8.03. Found: C, 56.81; H, 4.14; N, 10.13; S, 7.81.

*4.1.2.2. 4-[5-(6-Hydroxy-4-methoxybenzofuran-5-yl)-3-trifluoromethyl-1H-pyrazol-1-yl]benzene sulfonamide (**3b**).* Yield 60%, m.p. 192–193 °C IR (KBr, cm^{-1}): 3336, 3244 (NH_2), 3151 (OH), 1635 (C=N), 1334, 1161 (SO_2). ^1H NMR (DMSO-d_6) δ *ppm*: 2.49 (s, 2H, NH_2, exch. D_2O), 4.02 (s, 3H, OCH_3), 6.85 (s, 1H, H-7 benzofuran), 7.13 (d, 1H, H-3 benzofuran, J = 2.4 Hz), 7.33 (s, 1H, H-4 pyrazole), 7.56 (d, 1H, H-2 benzofuran, J = 2.4 Hz), 7.84 (d, 2H, H-2 and H-6 $ArSO_2NH_2$, J = 8.4 Hz), 8.06 (d, 2H, H-3 and H-5 $ArSO_2NH_2$, J = 8.7 Hz), 10.01 (s, 1H, OH, exch. D_2O). ^{13}C NMR (DMSO) δ: 60.19 (OCH_3), 92.95 (C-7), 105.18 (C-5), 105.83 (C-3), 110.18 (C-4 pyrazole), 112.15 (C-3a), 125.09 (C-3 and C-5 $ArSO_2NH_2$), 127.04 (C-2 and C-6 $ArSO_2NH_2$), 131.00 (CF_3), 140.77 (C-1 $ArSO_2NH_2$), 143.45 (C-4 $ArSO_2NH_2$), 144.64 (C-5 pyrazole), 147.43 (C-2), 151.87 (C-3 pyrazole), 154.51 (C-6), 156.64 (C-4), 157.54 (C-7a). MS, *m/z*: 454 [M^+ + 1]. Anal. Calcd. for $C_{19}H_{14}F_3N_3O_5S$ (453.39): C, 50.33; H, 3.11; N, 9.27; S, 7.07. Found: C, 50.60; H, 3.05; N, 8.81; S, 6.93.

Table 5
ADME of celecoxib and the newly synthesized compounds using mipc-Molinspiration Property Calculator.

Compound	MW	No. of H-bond donors	No. of H-bond acceptors	miLog*P*	No. of rotatable bonds	TPSA	No. of violations
Celecoxib	381.378	2	5	3.66	4	77.99	0
3c	462.49	3	9	2.62	5	133.49	0
3d	483.42	3	9	3.14	6	129.83	0
3e	492.51	3	10	2.61	6	142.72	1
9c	493.52	2	8	4.12	6	109.60	0
9d	543.52	2	8	4.87	7	109.60	1

MW: molecular weight.
miLog*P*: Octanol-water partition coefficient (predicted log*P* at Molinspiration).
TPSA: Topological polar surface area.

*4.1.2.3. 4-[5-(6-Hydroxy-4-methoxybenzofuran-5-yl)-3-(pyridin-3-yl)-1H-pyrazol-1-yl]benzene sulfonamide (**3c**).* Yield 55%, m.p. 124–126 °C IR (KBr, cm^{-1}): 3305, 3251 (NH_2), 3153 (OH), 1660 (C=N), 1334, 1153 (SO_2). ^1H NMR (DMSO-d_6) δ *ppm*: 2.13 (s, 2H, NH_2, exch. D_2O), 4.12 (s, 3H, OCH_3), 6.71 (s, 1H, H-7 benzofuran), 6.95 (d, 1H, H-3 benzofuran, $J = 2.1$ Hz), 7.06 (m, 1H, H-5 pyridine), 7.16 (d, 2H, H-2 and H-6 Ar–SO_2NH_2, $J = 8.1$ Hz), 7.31 (s, 1H, H-4 pyrazole), 7.56 (d, 1H, H-2 benzofuran, $J = 2.1$ Hz), 7.81 (d, 2H, H-3 and H-5 $ArSO_2NH_2$, $J = 8.1$ Hz), 8.60 (d, 1H, H-4 pyridine, $J = 7.5$ Hz), 8.80 (d, 1H, H-6 pyridine, $J = 7.5$ Hz), 9.40 (s, 1H, H-2 pyridine), 10.00 (s, 1H, OH exch. D_2O). MS, *m/z*: 462 [M^+]. Anal. Calcd. for $C_{23}H_{18}N_4O_5S$ (462.48): C, 59.73; H, 3.92; N, 12.11; S, 6.93. Found: C, 59.57; H, 3.80; N, 12.59; S, 6.69.

*4.1.2.4. 4-[5-(6-Hydroxy-4,7-dimethoxybenzofuran-5-yl)-3-trifluoromethyl-1H-pyrazol-1-yl]benzene sulfonamide (**3d**).* Yield 55%, m.p. 118–120 °C. IR (KBr, cm^{-1}): 3356, 3255 (NH_2), 3132 (OH), 1624 (C=N), 1338, 1134 (SO_2). ^1H NMR (DMSO-d_6.D_2O) δ *ppm*: 2.60 (s, 2H, NH_2, exch. D_2O), 3.95 (s, 3H, OCH_3), 4.10 (s, 3H, OCH_3), 6.85 (d, 1H, H-3 benzofuran, $J = 2.1$ Hz), 7.01 (d, 2H, H-2 and H-6 $ArSO_2$, $J = 8.4$ Hz), 7.20 (s, 1H, H-4 pyrazole), 7.65 (d, 1H, H-2 benzofuran, $J = 2.1$ Hz), 7.71 (d, 2H, H-3 and H-5 $ArSO_2$, $J = 8.7$ Hz), 10.51 (s, 1H, OH exch. D_2O). MS, *m/z*: 485 [$M^+ + 2$]. Anal. Calcd. for $C_{20}H_{16}F_3N_3O_6S$ (483.42): C, 49.69; H, 3.34; N, 8.69; S, 6.63. Found: C, 50.01; H, 3.72; N, 8.82; S, 6.50.

*4.1.2.5. 4-[5-(6-Hydroxy-4,7-dimethoxybenzofuran-5-yl)-3-(pyridin-3-yl)-1H-pyrazol-1-yl]benzene sulfonamide (**3e**).* Yield 65%, m.p. 154–155 °C. IR (KBr, cm^{-1}): 3336, 3267 (NH_2), 3124 (OH), 1643 (C=N), 1330, 1153 (SO_2). ^1H NMR (DMSO-d_6) δ *ppm*: 2.46 (s, 2H, NH_2, exch. D_2O), 3.85 (s, 3H, OCH_3), 4.08 (s, 3H, OCH_3), 6.85 (d, 1H, H-3 benzofuran, $J = 2.1$ Hz), 7.05–7.26 (m, 1H, H-5 pyridine), 7.45 (s, 1H, H-4 pyrazole), 7.51 (d, 2H, H-2 and H-6 Ar–SO_2NH_2, $J = 8.1$ Hz), 7.63 (d, 2H, H-3 and H-5 $ArSO_2NH_2$, $J = 8.1$ Hz), 7.87 (d, 1H, H-4 pyridine, $J = 7.5$ Hz), 8.27 (d, 1H, H-2 benzofuran, $J = 2.1$ Hz), 8.60 (d, 1H, H-6 pyridine, $J = 7.5$ Hz), 9.17 (s, 1H, H-2 pyridine), 9.99 (s, 1H, OH exch. D_2O). ^{13}C NMR (DMSO) δ: 61.02 (OCH_3), 61.81 (OCH_3), 95.93 (C-7), 105.48 (C-5), 106.55 (C-3), 110.72 (C-4 pyrazole), 112.49 (C-3a), 120.21 (C-2 and C-6 $ArSO_2NH_2$), 125.82 (C-5 pyridine), 128.95 (C-3 and C-5 $ArSO_2NH_2$), 130.44 (C-1 pyridine), 134.18 (C-6 pyridine), 138.01 (C-3 pyrazole), 141.45 (C-4 $ArSO_2NH_2$), 143.06 (C-1 $ArSO_2NH_2$), 144.99 (C-5 pyrazole), 146.00 (C-2), 147.00 (C-4), 148.68 (C-4 pyridine), 149.37 (C-7a), 150.45 (C-2 pyridine), 150.95 (C-6). MS, *m/z*: 493 [$M^+ + 1$]. Anal. Calcd. for $C_{24}H_{20}N_4O_6S$ (492.50): C, 58.53; H, 4.09; N, 11.38; S, 6.51. Found: C, 58.53; H, 3.92; N, 11.33; S, 6.65.

*4.1.3. General procedure for the synthesis of 2-(4-(un) substituted benzylidene)-4-methoxy-furano[3,2-f]benzofuran-3(2H)-one (**5a**,**b**)*

To a solution of compound **4a** or **4b** (5 mmol) in a mixture acetone (5 ml) and methanol (15 ml) was added 4 N sodium hydroxide (1.5 ml) and 30% hydrogen peroxide solution (2 ml). The reaction mixture was heated to boiling during 1 h. After standing for 24 h at room temperature, the formed precipitate was filtered off and crystallized from chloroform-acetone mixture. Compounds **5a**, **b** were yellow-orange crystals which had a negative ferric chloride reaction and were insoluble in alkali.

*4.1.3.1. 2-(4-Chlorobenzylidene)-4-methoxy-furano[3,2-f]benzofuran-3(2H)-one (**5b**).* Yield 85%, m.p. 229–231 °C. IR (KBr, cm^{-1}): 1697 (C=O). ^1H NMR (DMSO- d_6) δ *ppm*: 4.32 (s, 3H, OCH_3), 6.76 (s, 1H, H-7 benzofuran), 7.30 (d, 1H, H-3 benzofuran, $J = 2.1$ Hz), 7.50 (s, 1H, =CH–), 7.57 (d, 2H, H-3 and H-5 ArCl, $J = 9.0$ Hz), 7.70 (d, 1H, H-2 benzofuran, $J = 2.1$ Hz), 7.98 (d, 2H, H-2 and H-6 ArCl, $J = 9.0$ Hz). MS, *m/z*: 326 [M^+], 328 [$M^+ + 2$]. Anal. Calcd. for $C_{18}H_{11}ClO_4$ (326.73): C, 66.17; H, 3.39. Found: C, 66.39; H, 3.20.

*4.1.4. General procedure for the synthesis of (E)-3-(4-substituted phenyl)-1-(4,6-dimethoxybenzofuran-5-yl)prop-2-en-1-one (**7b**–**d**)*

The worm solution of 1-(4,6-dimethoxybenzofuran-5-yl)ethanone **6** (10 mmol, 2.2 g) and the appropriate aromatic aldehyde (11 mmol) in ethanol (10 ml) was treated with sodium hydroxide (30%, 5 ml). The obtained red solution was allowed to stand for 48 h at room temperature, and then it was diluted with water and acidified with acetic acid. The produced precipitate was filtered, dried and crystallized from ethanol to give orange to red crystals having negative ferric chloride reaction.

*4.1.4.1. (E)-3-(4-Chlorophenyl)-1-(4,6-dimethoxybenzofuran-5-yl) prop-2-en-1-one (**7b**).* Yield 76%, m.p. 152–154 °C. IR (KBr, cm^{-1}): 1685 (C=O). ^1H NMR (DMSO-d_6) δ *ppm*: 3.91 (s, 3H, OCH_3), 4.09 (s, 3H, OCH_3), 6.77 (s, 1H, H-7 benzofuran), 6.88 (d, 1H, H-3 benzofuran, $J = 2.1$ Hz), 6.98 (d, 1H, –CO–CH=CH–, $J = 15.9$ Hz), 7.35 (d, 2H, H-3 and H-5 ArCl, $J = 8.7$ Hz), 7.46 (d, 2H, H-2 and H-6 ArCl, $J = 8.7$ Hz), 7.54 (d, 1H, H-2 benzofuran, $J = 2.1$ Hz), 7.95 (d, 1H, –CO–CH=CH–, $J = 15.9$ Hz). MS, *m/z*: 342 [M^+], 344 [$M^+ + 2$]. Anal. Calcd. for $C_{19}H_{15}ClO_4$ (342.77): C, 66.58; H, 4.41. Found: C, 67.02; H, 4.47.

*4.1.4.2. (E)-3-(4-Fluorophenyl)-1-(4,6-dimethoxybenzofuran-5-yl) prop-2-en-1-one (**7c**).* Yield 70%, m.p. 138–140 °C. IR (KBr, cm^{-1}): 1681 (C=O). ^1H NMR (DMSO-d_6) δ *ppm*: 3.78 (s, 3H, OCH_3), 3.97 (s, 3H, OCH_3), 6.76 (s, 1H, H-7 benzofuran), 7.00 (d, 1H, H-3 benzofuran, $J = 2.1$ Hz), 7.16 (d, 1H, –CO–CH=CH–, $J = 16.5$ Hz), 7.31 (d, 2H, H-3 and H-5 ArF, $J = 9.0$ Hz), 7.45 (d, 1H, H-2 benzofuran, $J = 2.1$ Hz), 7.82 (d, 2H, H-2 and H-6 ArF, $J = 9.3$ Hz), 7.98 (d, 1H, –CO–CH=CH–, $J = 15.9$ Hz). MS, *m/z*: 326 [M^+]. Anal. Calcd. for $C_{19}H_{15}FO_4$ (326.32): C, 69.93; H, 4.63. Found: C, 69.64; H, 4.46.

*4.1.4.3. (E)-3-(4-Trifluoromethyl phenyl)-1-(4,6-dimethoxybenzofuran-5-yl)prop-2-en-1-one (**7d**).* Yield 60%, m.p.

146–148 °C. IR (KBr, cm^{-1}): 1701 (C=O). ^1H NMR (DMSO-d_6) δ *ppm*: 3.97 (s, 3H, OCH_3), 4.04 (s, 3H, OCH_3), 6.97 (s, 1H, H-7 benzofuran), 7.07 (d, 1H, H-3 benzofuran, $J = 2.1$ Hz), 7.13 (d, 2H, H-2 and H-6 $ArCF_3$, $J = 9.3$ Hz), 7.54 (d, 1H, H-2 benzofuran, $J = 2.1$ Hz), 7.61 (d, 1H, −CO−CH=CH−, $J = 16.8$ Hz), 7.88 (d, 2H, H-3 and H-5 $ArCF_3$, $J = 9.3$ Hz), 8.30 (d, 1H, −CO−CH=CH-, $J = 15.9$ Hz). MS, *m/z*: 376 [M^+]. Anal. Calcd. for $C_{20}H_{15}F_3O_4$ (376.33): C, 63.83; H, 4.02. Found: C, 63.54; H, 3.95.

4.1.5. General procedure for the synthesis of [3-(4-substituted phenyl)oxiran-2-yl](4,6-dimethoxybenzofuran-5-yl)methanone (**8a**–**d**)

A solution of the appropriate chalcone **7a**–**d** (10 mmol) in acetone (10 ml) and methyl alcohol (30 ml) was mixed with 4 N sodium hydroxide (3 ml) followed by drop wise addition of hydrogen peroxide (30%, 5 ml). The solution was shaken and heated to the boiling point during 1 h; then allowed to stand overnight at room temperature, the reaction mixture became lighter in color. Crystals of the α-keto epoxide deposited and extracted with diethyl ether (3 × 5 ml), the ethereal extracts were combined and evaporated. The residue was crystallized from petroleum ether to give yellowish-white to white powder.

*4.1.5.1. (4,6-Dimethoxybenzofuran-5-yl)(3-phenyloxiran-2-yl)methanone (**8a**).* Yield 64%, m.p. 102–104 °C. IR (KBr, cm^{-1}): 1693 (C=O). ^1H NMR (DMSO- d_6) δ *ppm*: 3.80 (d, 1H, H-3 oxirane, $J = 2.7$ Hz), 3.99 (s, 3H, OCH_3), 4.07 (s, 3H, OCH_3), 4.20 (d, 1H, H-2 oxirane, $J = 2.7$ Hz), 6.76 (s, 1H, H-7 benzofuran), 6.98 (d, 1H, H-3 benzofuran, $J = 2.1$ Hz), 7.13–7.54 (m, 5H, ArH), 7.88 (d, 1H, H-2 benzofuran, $J = 2.4$ Hz). MS, *m/z*: 324 [M^+]. Anal. Calcd. for $C_{19}H_{16}O_5$ (324.33): C, 70.36; H, 4.97. Found: C, 70.80; H, 4.51.

*4.1.5.2. [3-(4-Chlorophenyl)oxiran-2-yl](4,6-dimethoxybenzofuran-5-yl)methanone (**8b**).* Yield 72%, m.p. 132–134 °C. IR (KBr, cm^{-1}): 1701 (C=O). ^1H NMR ($CDCl_3$) δ *ppm*: 3.79 (s, 3H, OCH_3), 3.94 (d, 1H, H-3 oxirane, $J = 2.4$ Hz), 4.02 (d, 1H, H-2 oxirane, $J = 2.4$ Hz), 4.12 (s, 3H, OCH_3), 6.77 (s, 1H, H-7 benzofuran), 6.86 (d, 1H, H-3 benzofuran, $J = 2.1$ Hz), 7.34 (d, 2H, H-2 and H-6 ArCl, $J = 8.4$ Hz), 7.49 (d, 1H, H-2 benzofuran, $J = 2.4$ Hz), 8.02 (d, 2H, H-3 and H-5 ArCl, $J = 8.4$ Hz). MS, *m/z*: 358 [M^+], 360 [$M^+ + 2$]. Anal. Calcd. For $C_{19}H_{15}ClO_5$ (358.77): C, 63.61; H, 4.21. Found: C, 63.61; H, 3.96.

*4.1.5.3. [3-(4-Fluorophenyl)oxiran-2-yl](4,6-dimethoxybenzofuran-5-yl)methanone (**8c**).* Yield 65%, m.p. 118–120 °C. IR (KBr, cm^{-1}): 1701 (C=O). ^1H NMR ($CDCl_3$) δ *ppm*: 3.83 (s, 3H, OCH_3), 3.88 (d, 1H, H-3 oxirane, $J = 2.7$ Hz), 3.97 (d, 1H, H-2 oxirane, $J = 2.7$ Hz), 4.10 (s, 3H, OCH_3), 6.78 (s, 1H, H-7 benzofuran), 6.88 (d, 1H, H-3 benzofuran, $J = 2.1$ Hz), 7.46 (d, 2H, H-3 and H-5 ArF, $J = 7.8$ Hz), 7.65 (d, 1H, H-2 benzofuran, $J = 2.4$ Hz), 7.65 (d, 2H, H-2 and H-6 ArF, $J = 7.8$ Hz). MS, *m/z*: 342 [M^+]. Anal. Calcd. For $C_{19}H_{15}FO_5$ (342.32): C, 66.66; H, 4.42. Found: C, 66.71; H, 4.30.

*4.1.5.4. {3-[4-(Trifluoromethyl)phenyl]oxiran-2-yl}(4,6-dimethoxybenzofuran-5-yl)methanone (**8d**).* Yield 60%, m.p. 126–128 °C. IR (KBr, cm^{-1}): 1705 (C=O). ^1H NMR ($CDCl_3$) δ *ppm*: 3.82 (s, 3H, OCH_3), 3.93 (d, 1H, H-3 oxirane, $J = 2.4$ Hz), 4.05 (s, 3H, OCH_3), 4.20 (d, 1H, H-2 oxirane, $J = 2.4$ Hz), 6.84 (s, 1H, H-7 benzofuran), 6.90 (d, 1H, H-3 benzofuran, $J = 2.4$ Hz), 7.32 (d, 2H, H-2 and H-6 $ArCF_3$, $J = 8.1$), 7.54 (d, 1H, H-2 benzofuran, $J = 2.4$ Hz), 7.63 (d, 2H, H-3 and H-5 $ArCF_3$, $J = 8.1$ Hz). MS, *m/z*: 392 [M^+]. Anal. Calcd. For $C_{20}H_{15}F_3O_5$ (392.33): C, 61.23; H, 3.85. Found: C, 61.55; H, 3.88.

4.1.6. General procedure for the synthesis of 4-[5-aryl-3-(4,6-dimethoxybenzofuran-5-yl)-1H-pyrazol-1-yl]benzene sulfonamide derivatives (**9a**–**d**)

The oxirane derivative **8a**–**d** (10 mmol) was added to a stirred solution of *p*-sulfamoylphenylhydrazine hydrochloride (11 mmol, 2.46 g) in ethanol (10 ml) and acetic acid (0.5 ml). The reaction mixture was stirred at reflux for 6 h. After cooling to room temperature, the reaction mixture was concentrated under vacuum. The residue was taken up with ethyl acetate. The organic layer was washed several times with water, dried over anhydrous $MgSO_4$ and evaporated under vacuum. The residue was crystallized from ethanol.

*4.1.6.1. 4-[3-(4,6-Dimethoxybenzofuran-5-yl)-5-phenyl-1H-pyrazol-1-yl]benzene sulfonamide (**9a**).* Yield 64%, m.p. 144–145 °C. IR (KBr, cm^{-1}): 3387, 3263 (NH_2), 1624 (C=N), 1350, 1153 (SO_2). ^1H NMR (DMSO-d_6) δ *ppm*: 1.40 (s, 2H, NH_2, exch. D_2O), 4.02 (s, 3H, OCH_3), 4.22 (s, 3H, OCH_3), 6.95 (s, 1H, H-7 benzofuran), 7.12 (d, 1H, H-3 benzofuran, $J = 2.1$ Hz), 7.19 (s, 1H, H-4 pyrazole), 7.26–7.40 (m, 5H, ArH), 7.60 (d, 2H, H-2 and H-6 $ArSO_2NH_2$, $J = 8.7$ Hz), 7.80 (d, 1H, H-2 benzofuran, $J = 2.1$ Hz), 7.95 (d, 2H, H-3 and H-5 $ArSO_2NH_2$, $J = 8.4$ Hz). MS, *m/z*: 474 [$M^+ - 1$]. Anal. Calcd. for $C_{25}H_{21}N_3O_5S$ (475.52): C, 63.15; H, 4.45; N, 8.84; S, 6.74. Found: C, 63.08; H, 4.28; N, 8.84; S, 6.74.

*4.1.6.2. 4-[5-(4-Chlorophenyl)-3-(4,6-dimethoxybenzofuran-5-yl)-1H-pyrazol-1-yl]benzene sulfonamide (**9b**).* Yield 75%, m.p. 156–158 °C. IR (KBr, cm^{-1}): 3383, 3271 (NH_2), 1630 (C=N), 1334, 1153 (SO_2). ^1H NMR ($CDCl_3$) δ *ppm*: 1.26 (s, 2H, NH_2, exch. D_2O), 3.85 (s, 3H, OCH_3), 4.06 (s, 3H, OCH_3), 6.75 (s, 1H, H-7 benzofuran), 6.83 (d, 1H, H-3 benzofuran, $J = 2.1$ Hz), 6.89 (s, 1H, H-4 pyrazole), 6.93 (d, 2H H-3 and H-5 ArCl, $J = 9.0$ Hz), 6.98 (d, 2H, H-2 and H-6 $ArSO_2NH_2$, $J = 8.7$ Hz), 7.33 (d, 2H, H-3 and H-5 $ArSO_2NH_2$, $J = 8.7$ Hz), 7.44 (d, 2H, H-2 and H-6 ArCl, $J = 9.0$ Hz), 7.60 (d, 1H, H-2 benzofuran, $J = 2.1$ Hz). MS, *m/z*: 509 [M^+], 511 [$M^+ + 2$]. Anal. Calcd. for $C_{25}H_{20}ClN_3O_5S$ (509.96): C, 58.88; H, 3.95; N, 8.24. Found: C, 59.38; H, 4.06; N, 8.58.

*4.1.6.3. 4-[5-(4-Fluorophenyl)-3-(4,6-dimethoxybenzofuran-5-yl)-1H-pyrazol-1-yl]benzene sulfonamide (**9c**).* Yield 60%, m.p. 175–177 °C. IR (KBr, cm^{-1}): 3361, 3261 (NH_2), 1620 (C=N), 1334, 1155 (SO_2). ^1H NMR (DMSO-d_6) δ *ppm*: 1.25 (s, 2H, NH_2, exch. D_2O), 3.79 (s, 3H, OCH_3), 4.08 (s, 3H, OCH_3), 6.80 (s, 1H, H-7 benzofuran), 7.06 (d, 1H, H-3 benzofuran, $J = 2.1$ Hz), 7.14 (d, 2H, H-3 and H-5 ArF, $J = 9.3$ Hz), 7.20 (d, 2H, H-2 and H-6 ArF, $J = 9.0$ Hz), 7.41 (d, 2H, H-2 and H-6 $ArSO_2NH_2$, $J = 8.4$), 7.60 (d, 2H, H-3 and H-5 $ArSO_2NH_2$, $J = 8.4$ Hz), 7.89 (d, 1H, H-2 benzofuran, $J = 1.8$ Hz), 8.30 (s, 1H, H-4 pyrazole). MS, *m/z*: 493 [M^+]. Anal. Calcd. for $C_{25}H_{20}FN_3O_5S$ (493.51): C, 60.84; H, 4.08; N, 8.51; S, 6.50. Found: C, 61.04; H, 3.95; N, 8.32; S, 6.30.

*4.1.6.4. 4-[5-(4-Trifluoromethylphenyl)-3-(4,6-dimethoxybenzofuran-5-yl)-1H-pyrazol-1-yl]benzene sulfonamide (**9d**).* Yield 58%, m.p. 185–186 °C. IR (KBr, cm^{-1}): 3387, 3275 (NH_2), 1620 (C=N), 1327, 1157 (SO_2). ^1H NMR (DMSO-d_6) δ *ppm*: 1.25 (s, 2H, NH_2, exch. D_2O), 3.86 (s, 3H, OCH_3), 4.02 (s, 3H, OCH_3), 6.90 (s, 1H, H-7 benzofuran), 7.00 (d, 1H, H-3 benzofuran, $J = 2.1$ Hz), 7.15 (d, 2H, H-2 and H-6 $ArCF_3$, $J = 9.3$ Hz), 7.30 (d, 2H, H-3 and H-5 $ArCF_3$, $J = 9.3$ Hz), 7.50 (s, 1H, H-4 pyrazole), 7.60 (d, 1H, H-2 benzofuran, $J = 1.8$ Hz), 7.70 (d, 2H, H-2 and H-6 $ArSO_2NH_2$, $J = 8.7$ Hz), 7.85 (d, 2H, H-3 and H-5 $ArSO_2NH_2$, $J = 8.7$ Hz). ^{13}C NMR (DMSO) δ: 56.06 (OCH_3), 56.31 (OCH_3), 89.53 (C-7), 102.06 (C-5), 105.17 (C-3), 111.19 (C-3a), 115.20 (C-4 pyrazole), 120.63 (C-2 and C-6 $ArSO_2NH_2$), 125.58 (C-3 and C-5 $ArCF_3$), 126.92 (CF_3), 127.59 (C-2 and C-6 $ArCF_3$), 129.09 (C-3 and C-5 $ArSO_2NH_2$), 129.92 (C-4 $ArCF_3$),

130.02 (C-1 $ArCF_3$), 136.47 (C-4 $ArSO_2NH_2$), 142.97 (C-1 $ArSO_2NH_2$), 144.30 (C-5 pyrazole), 146.00 (C-2), 152.00 (C-6), 156.00 (C-4), 158.00 (C-7a), 160.36 (C-3 pyrazole). MS, *m/z*: 543 [M^+]. Anal. Calcd. for $C_{26}H_{20}F_3N_3O_5S$ (543.51): C, 57.46; H, 3.71; N, 7.73; S, 5.90. Found: C, 57.90; H, 3.86; N, 7.66; S, 6.27.

4.2. Pharmaco-biological evaluation

4.2.1. In vitro cyclooxygenase (COX) inhibition assay

The ability of the test compounds to inhibit ovine COX-1 and human recombinant COX-2 was determined using an enzyme immunoassay (EIA) (kit catalog number 560131, Cayman Chemical, Ann Arbor, MI, USA) according to the manufacturer's instructions. Cyclooxygenase catalyzes the first step in the biosynthesis of arachidonic acid (AA) to PGH_2. $PGF_{2\alpha}$, produced from PGH_2 by reduction with stannous chloride, is measured by enzyme immunoassay (ACE™ competitive EIA). Stock solutions of test compounds were dissolved in a minimum volume of DMSO. Briefly, to a series of supplied reaction buffer solutions (950 μL, 0.1 M Tris–HCl pH 8.0 containing 5 mM EDTA and 2 mM phenol) with either COX-1 or COX-2 (10 μL) enzyme in the presence of heme (10 μL) were added 20 μL of various concentrations of test drug solutions (0, 0.01, 0.1, 1, 10 and 50 μM in a final volume of 1 ml). These solutions were incubated for a period of 10 min at 37 °C, after which 10 μL of AA (100 μM) solution were added and the COX reaction was stopped by the addition of 50 μL of 1 M HCl after 2 min. $PGF_{2\alpha}$, produced from PGH_2 by reduction with stannous chloride was measured by enzyme immunoassay. This assay is based on the competition between PGs and a PG-acetyl cholinesterase conjugate (PG tracer) for a limited amount of PG antiserum. The amount of PG tracer, that is, able to bind to the PG antiserum is inversely proportional to the concentration of PGs in the wells since the concentration of PG tracer is held constant while the concentration of PGs varies. This antibody–PG complex binds to a mouse anti-rabbit monoclonal antibody that had been previously attached to the well. The plate is washed to remove any unbound reagents and then Elman's reagent, which contains the substrate to acetylcholine esterase, is added to the well. The product of this enzymatic reaction produces a distinct yellow color that absorbs at 410 nm. The intensity of this color, determined spectrophotometrically, is proportional to the amount of PG tracer bound to the well, which is inversely proportional to the amount of PGs present in the well during the incubation: Absorbance α [Bound PG Tracer] α1/PGs. Percent inhibition was calculated by the comparison of compound treated to various control incubations. The concentration of the test compound causing 50% inhibition (IC_{50}, μM) was calculated from the concentration–inhibition response curve (duplicate determinations).

4.2.2. In vivo anti-inflammatory activity

All the animal experiments were performed according to protocols approved by the Animal Use and Care Committee of University of Cairo, Egypt.

4.2.2.1. Animals. Adult male Wister albino rats (120–150 g) were used to study the anti-inflammatory activity and ulcerogenic liabilities. The animals (five per cage) were maintained under standard laboratory conditions (light period of 12 h/day and temperature 27 ± 2 °C), with access to food and water. The experimental procedures were carried out in strict compliance with the Institutional Animal Ethics Committee regulations. All experiments were performed in the morning according to the guidelines for the care of laboratory animals [53].

4.2.2.2. Formalin induced rat paw edema. Anti-inflammatory activity study for the prepared compounds was determined in vivo by the standard formalin-induced paw edema method in rats [32]. Wister albino rats were divided into seven groups of five animals each. Thickness of the left hind paw of each rat was measured, in millimeters using Vernier caliper, before any drug administration (0 h). The first group was kept as negative control given 10% DMSO aqueous solution (v/v). Celecoxib was orally administered to the second group as a reference standard (50 mg/kg). The tested compounds **3c**, **3d**, **3e**, **9c** and **9d** in the form of 10% DMSO aqueous solutions were given *via* oral route to the rest groups at a dose of 50 mg/kg body weight, treatments began 1 h before induction of inflammation. Paw edema was induced by subcutaneous injection of 2.5% formalin solution (0.1 ml/rat) into the right hind paw of each rat. Paw thickness of each rat was measured after 30 min, 1, 2 and 3 h of formalin injection using Vernier caliper. The edema thickness (mm) was calculated by subtracting the zero-hour reading from each time reading. The anti-inflammatory activity was expressed as percentage inhibition of edema thickness in treated animals in comparison with the control group, Table 1

$$\text{Edema inhibition}\% = V_c - V_t/V_c \times 100$$

Where, V_c and V_t are the thickness of edema for the control and drug-treated animal groups.

4.2.3. Ulcerogenic liability

The ulcerogenic effect of the most active compounds **3c**, **3d**, **3e**, **9c** and **9d** as well as celecoxib and ibuprofen was evaluated according to Meshali's method [33]. Forty adult male albino rats were used in this study and divided into 8 groups. The animals were fasted 18 h before drug administration. The first group received 10% DMSO aqueous solution (v/v) and kept as control the second group received celecoxib in a dose of 50 mg/kg, while the third group received ibuprofen in a dose of 25 mg/kg. The other groups received **3c**, **3d**, **3e**, **9c** and **9d** in a dose 50 mg/kg. Animals were fed 2 h after administration of the drug. Rats received the given dose orally for three successive days. Two hours following the last dose, rats were scarified; the stomach of each rat was removed, opened along the greater curvature and rinsed with 0.9% sodium chloride. The stomach was stretched; by pins; on a corkboard. Examination with a magnifying lens (10 xs) was done for the presence of ulcers and erosions. The ulcer index was calculated according to Robert's method [34]. The degree of ulcerogenic effect was expressed in term of the percentage incidence of ulcers in each group of animals divided by 10, the average number of ulcers per stomach and the average severity of ulcers (ulcer score) by visual observation. The ulcer scores were: 0 = no ulcer, 1 = mucosal erythema only, 2 = mild mucosal edema, slight bleeding or slight erosion, 3 = moderate edema, bleeding ulcers or erosions, 4 = sever ulceration, erosions, edema and tissue necrosis. The ulcer index is the value that result from the sum of the above three values.

4.2.4. Statistical analysis

The results were expressed as Mean ± S.E. "standard error". The significant difference among the groups was assessed using one way analysis of variance (ANOVA) followed by Dunnett's test at $p < 0.01$.

4.3. Molecular modeling

All molecular modeling calculation and docking studies were carried out using Molecular Operating Environment MOE version 2008.10 [37]. The target compounds were drawn on MOE. The structures were subjected to energy minimization using Hamiltonian-Force Field-MMFF94x. The most stable conformers for each compound were retained and partial charges were calculated.

The X-ray crystal structure of COX-2 enzyme in complex with SC-558, PDB ID code 6COX was recovered from RSCB protein data bank [38]. The enzyme was prepared for docking as follows: 1) The Co-crystallized ligand and water molecules were removed. 2) The enzyme was 3D protonated, where hydrogen atoms were added at their standard geometry, the partial charges were computed and the system was optimized. Flexible ligand- rigid receptor docking of the most stable conformers was done with MOE-DOCK using triangle matcher as placement method and London dG as a scoring function. The obtained poses were subjected to force field refinement using the same scoring function. Ten of the most stable docking models for each ligand were retained with the best scored conformation. In order to validate the docking procedure, SC-558 was docked into the active site of 6COX. The docking results show that the compound exhibit similar interaction reported in literature with RMSD = 0.218 Å.

References

[1] D.A. Williams, T.L. Lemke, Non-steroidal anti-inflammatory drugs, in: D.A. Williams (Ed.), Foye's Principles of Medicinal Chemistry, fifth ed., Lippincott Williams & Wilkins, 2002, pp. 751–793.
[2] P. Gund, T.Y. Shen, Journal of Medicinal Chemistry 20 (1977) 1146–1152.
[3] J.Y. Jouzeau, B. Terlain, A. Abid, E. Nedelec, P. Netter, Drugs 53 (1997) 563–582.
[4] H. Yoshimura, S. Sekine, H. Adachi, Y. Uematsu, A. Mitani, N. Futaki, N. Shimizu, Protein Expression and Purification 80 (2011) 41–46.
[5] B. Yao, J. Xu, R.C. Harris, M.Z. Zhang, American Journal of Physiology – Renal Physiology 294 (2008) 433–439.
[6] H. Haruna, T. Shimizu, Y. Ohtsuka, Y. Yarita, T. Fujii, T. Kudo, Y. Yamashiro, Pediatrics International 50 (2008) 1–6.
[7] S. Yoshida, M. Ujiki, X.Z. Ding, C. Pelman, M.S. Talamonti, R.H. Bell, W. Denham, T.E. Adrian, Molecular Cancer 4 (2005) 27.
[8] M.G. Perrone, A. Scilimati, L. Simone, P. Vitale, Current Medicinal Chemistry 17 (2010) 3769–3805.
[9] P. Vitale, S. Tacconelli, M.G. Perrone, P. Malerba, L. Simone, A. Scilimati, A. Lavecchia, M. Dovizio, E. Marcantoni, A. Bruno, P. Patrignani, Journal of Medicinal Chemistry 56 (2013) 4277–4299.
[10] K.G. Peri, P. Hardy, D.Y. Li, D.R. Varma, S. Chemtob, Journal of Biological Chemistry 270 (1995) 24615–24620.
[11] A.L. Sampaio, J. Dalli, V. Brancaleone, F. D'Acquisto, M. Perretti, C. Wheatley, Mediators of Inflammation 2013 (2013) 741804.
[12] R. Calvello, M.A. Panaro, M.L. Carbone, A. Cianciulli, M.G. Perrone, P. Vitale, P. Malerba, A. Scilimati, Pharmacological Research 65 (2012) 137–148.
[13] L.A. Garcia-Rodriguez, S. Hernández-Diaz, Epidemiology 14 (2003) 240–246.
[14] C.H. Ruan, S.P. So, K.H. Ruan, Life Sciences 88 (2011) 24–30.
[15] M. Khan, A. Fraser, Irish Medical Journal 105 (2012) 119–121.
[16] W.B. Whyte, G. Faich, J.S. Borer, R.W. Makuch, American Journal of Cardiology 92 (2003) 411–418.
[17] N.M. Davies, A.J. McLachlan, R.O. Day, K.M. Williams, Clinical Pharmacokinetics 38 (2000) 225–242.
[18] J. Castellsague, N. Riera-Guardia, B. Calingaert, C. Varas-Lorenzo, A. Fourrier-Reglat, F. Nicotra, M. Sturkenboom, S. Perez-Gutthann, Drug Safety 35 (2012) 1127–1146.
[19] A.S. Kalgutkar, B.C. Crews, S.W. Rowlinson, A.B. Marnett, K.R. Kozak, R.P. Remmel, L.J. Marnett, Proceedings of the National Academy of Sciences of the United States of America 97 (2000) 925–930.
[20] L. Di Nunno, P. Vitale, A. Scilimati, S. Tacconelli, P. Patrignani, Journal of Medicinal Chemistry 47 (2004) 4881–4890.
[21] T.D. Penning, J.J. Talley, S.R. Bertenshaw, J.S. Carter, P.W. Collins, S. Docter, M.J. Graneto, L.F. Lee, J.W. Malecha, J.M. Miyashiro, R.S. Rogers, D.J. Rogier, S.S. Yu, G.D. Anderson, E.G. Burton, J.N. Cogburn, S.A. Gregory, C.M. Koboldt, W.E. Perkins, K. Seibert, A.W. Veenhuizen, Y.Y. Zhang, P.C. Isakson, Journal of Medicinal Chemistry 40 (1997) 1347–1365.
[22] O.L. Lorens, J.J. Perez, A. Palomer, D. Mauleon, Journal of Molecular Graphics and Modelling 20 (2002) 359–371.
[23] M. Zheng, Z. Zhang, W. Zhu, H. Liu, X. Luo, K. Chen, H. Jiang, Bioorganic and Medicinal Chemistry 14 (2006) 3428–3437.
[24] J.M. Janusz, P.A. Young, J.M. Ridgeway, M.W. Scherz, K. Enzweiler, L.I. Wu, L. Gan, J. Chen, D.E. Kellstein, S.A. Green, J.L. Tulich, T. Rosario-Jansen, I.J. Magrisso, K.R. Wehmeyer, D.L. Kuhlenbeck, T.H. Eichhold, R.L. Dobson, Journal of Medicinal Chemistry 41 (1998) 3515–3529.
[25] R. Deshpande, M. Bhagawan Raju, S. Parameshwar, S.M. Shanth Kumar, S. Appalaraju, S. Manjunath, S.M. Yelagatti, American Journal of Chemistry 2 (2012) 115–120.
[26] G.S. Hassan, G.A. Soliman, European Journal of Medicinal Chemistry 45 (2010) 4104–4112.
[27] F.A. Ragab, G.S. Hassan, H.A. Yossef, H.A. Hashem, European Journal of Medicinal Chemistry 42 (2007) 1117–1127.
[28] G.O. Dengiz, F. Odabasoglu, Z. Halici, H. Suleyman, E. Cadirci, Y. Bayir, Archives of Pharmacal Research 30 (2007) 1426–1434.
[29] T.A. Geissman, D.K. Fukushima, Journal of the American Chemical Society 70 (1948) 1686–1689.
[30] E. Weitz, A. Scheffer, Berichte 54 (1921) 2327–2344.
[31] Y. Apeloig, M. Karni, Z. Rapoport, Journal of the American Chemical Society 105 (1983) 2784–2793.
[32] R. Turner, Screening Method in Pharmacology. Anti-inflammatory Agent 13, Academic Press New York, London, 1965, p. 158.
[33] M. Meshali, E. El-Sabbah, A. Foda, Acta Pharmaceutica Technologica 29 (1983) 217–230.
[34] A. Robert, J.E. Nezamis, J.P. Phillips, Gastroenterology 55 (1968) 481–487.
[35] E.J. Freireich, E.A. Gehan, D.P. Rall, L.H. Schmidt, H.E. Skipper, Cancer Chemotherapy Reports 50 (1966) 219–244.
[36] J.L. Wang, D. Limburg, M.J. Graneto, J. Springer, J.R. Hamper, S. Liao, J.L. Pawlitz, R.G. Kurumbail, T. Maziasz, J.J. Talley, J.R. Kiefer, J. Carter, Bioorganic & Medicinal Chemistry Letters 20 (2010) 7159–7163.
[37] MOE, Chemical Computing Group, Inc., Montreal, http://www.chemcomp.com.
[38] R.G. Kurumbail, A.M. Stevens, J.K. Gierse, J.J. McDonald, R.A. Stegeman, J.Y. Pak, D. Gildehaus, J.M. Miyashiro, T.D. Penning, K. Seibert, P.C. Isakson, W.C. Stallings, Nature 384 (1996) 644–648.
[39] S.W. Rowlinson, J.R. Kiefer, J.J. Prusakiewicz, J.L. Pawlitz, K.R. Kozak, A.S. Kalgutkar, W.C. Stallings, R.G. Kurumbail, L.J. Marnett, Journal of Biological Chemistry 46 (2003) 45763–456769.
[40] A. DerHovanessian, J.B. Doyon, A. Jain, P.R. Rablen, A.M. Sapse, Org. Lett. 1 (1999) 1359–1362.
[41] Laurent Schaeffer, in: C.,G. Wermuth (Ed.), The Role of Functional Groups in Drug Receptor Interaction; The Practice of Medicinal Chemistry, third ed., Elsevier Ltd, 2008, pp. 464–479.
[42] P.N. Rao, Q.H. Chen, E.E. Knaus, Journal of Medicinal Chemistry 49 (2006) 1668–1683.
[43] Y. Harrak, G. Casula, J. Basset, G. Rosell, S. Plescia, D. Raffa, M.G. Cusimano, R. Pouplana, M.D. Pujol, Journal of Medicinal Chemistry 53 (2010) 6560–6571.
[44] Molinspiration Cheminformatics (http://www.molinspiration.com/cgi-bin/properties).
[45] C.A. Lipinski, F. Lombardo, B.W. Dominy, P.J. Feeney, Advanced Drug Delivery Reviews 46 (2001) 3–26.
[46] P.R. Duchowicz, A. Talevi, C. Bellera, L.E. Bruno-Blanch, E.A. Castro, Bioorganic and Medicinal Chemistry 15 (2007) 3711–3719.
[47] D.B. Jack, J.L. Hawker, L. Rooney, M. Beerahee, J. Lobo, P. Patel, Journal of Chromatography 452 (1988) 257–264.
[48] E. Spath, W. Gruber, Ber 71 (1938) 106–113.
[49] A. Schönberg, A. Sina, Journal of the American Chemical Society 72 (1950) 1611–1616.
[50] A. Schönberg, N. Badran, N.A. Starkowsky, Journal of the American Chemical Society 77 (1955) 5430–5431.
[51] A. Schönberg, N. Badran, N.A. Starkowsky, Journal of the American Chemical Society 75 (1953) 4992–4995.
[52] O.M. Abdel Hafez, K.H.M. Ahmed, E.E. Haggag, Molecules 6 (2001) 396–405.
[53] M. Zimmermann, Pain 6 (1983) 109–110.